Effect of Transmission Fiber on Chaos Communication System Based on Erbium-Doped Fiber Ring Laser

Fan Zhang and Pak L. Chu, *Member, IEEE, Fellow, OSA*

***Abstract*—We report a numerical study on the deterioration of eye opening penalty (EOP) and bit error rate (BER) of the received message from a communication system based on chaos generated in erbium-doped fiber ring laser (EDFRL) under the influence of amplifier noise, transmission fiber dispersion, and nonlinearity. Three different transmission fibers with practical parameters are considered. We find that in order to realize high-bit-rate chaotic communication, the residual fiber dispersion should be kept as small as possible. Furthermore, if the transmission power is optimized to balance the effect of amplifier noise and fiber nonlinearity, a message with bit rate on the order of several gigabits/second can be transmitted over hundreds of kilometers with acceptable BER deterioration. A comparison between open- and closed-loop structures is also conducted. Moreover, we find that the maximum bit rate is limited by the bandwidth of the chaos determined by the nonlinearity of the fiber ring laser and the laser configuration. It is possible to optimize these parameters to provide the maximum chaos bandwidth and hence the maximum message bit rate.**

***Index Terms*—Chaos, encoded communications, erbium-doped fiber laser, fiber nonlinearity, fiber propagation, secure communication.**

I. Introduction

SECURE communication using chaos as a carrier has been widely studied since the discovery of synchronized chaos [1]. Recently, with the observation of synchronized chaos in lasers, such as Nd:YAG laser [2], CO_2 laser [3], semiconductor laser [4], and erbium-doped fiber ring laser (EDFRL) [5], optical secure communication has received considerable attention due to the potential huge bandwidth. EDFRL is especially attractive since its lasing wavelength is near the minimum attenuation of the fiber. The common methods of introducing signal into the chaotic communication are message masking [6] and chaos modulation [7]. In the first method, the message is just added to the chaotic pulse stream. In the second method, the message is used to drive the chaotic dynamics of the laser. Obviously, this second approach provides enhanced security over the first one. To retrieve the message at the receiver, the modulated chaotic pulse train is coupled to another near-identical chaotic system. In this case, the receiver generates a chaotic pulse train synchronized to the transmitter chaos. The message is then recovered by canceling the two chaos trains against each other.

Manuscript received May 5, 2003; revised September 2, 2003. This work was supported by the Hong Kong government under CERG Grant 9040707.

The authors are with the Optoelectronics Research Centre, City University of Hong Kong, Kowloon, Hong Kong, China (e-mail: eepchu@cityu.edu.hk).

Digital Object Identifier 10.1109/JLT.2003.821721

The chaotic dynamics of EDFRL and its application to communications have been investigated both theoretically and experimentally [5]–[12]. Abarbanel *et al.* [8] developed a theoretical model of EDFRL and showed that a chaotic oscillation can achieve a bandwidth of at least several gigahertz. The chaotic behavior was found to arise from the nonlinear Kerr effect. Luo and Chu [5] and Lewis *et al.* [9] have studied the synchronization robustness when the corresponding parameters in the transmitter and receiver are mismatched. Luo *et al.* [10] demonstrated that a sinusoidal signal at 1 GHz could be transmitted and recovered in a chaos communication system. VanWiggeren *et al.* [12] realized chaotic EDFRL communication over a transmission single-mode fiber of 35 km and digital message at 250 Mb/s.

To construct a practical chaos communication system, we need to take into account many factors. For example, the maximum message bit rate will be limited by the bandwidth of the chaos train and the characteristics of the transmission fiber such as its length, dispersion, nonlinearity, etc. Very little has been reported on these aspects, although the bit constraints caused by long-distance transmission in a chaotic communication system based on semiconductor laser has been studied [13].

In this paper, we provide a detailed numerical study of transmission degradation of the retrieved message from a chaotic carrier generated by an erbium-doped fiber ring laser. The digital message is introduced into the transmitter chaos through chaotic modulation [7], [12], i.e., the second approach described in the previous paragraph. The encoded chaotic pulse train is then transmitted to the receiver through a conventional transmission fiber. The propagation along this transmission fiber is described by the nonlinear Schrödinger equation by taking into account the fiber dispersion and nonlinearity. The transmission distance is several hundred kilometers.

This paper is outlined as follows. In Section II, we describe the model used for the transmitter (receiver) and the transmission fiber. Also, we characterize the chaotic modulation method. In Section III, we study eye opening penalty (EOP) degradation at different bit rates due to amplifier noise, fiber dispersion, and nonlinearity. The effect of electrical filters is also discussed. Then in Section IV, we demonstrate bit error rate (BER) performance in three different transmission fibers. In Section V, chaotic communication employing the closed-loop structure is examined and compared with the open-loop structure. In Section VI, the available bandwidth of EDFRL and the bit barrier of chaotic communication are discussed. Finally, in Section VII we give a summary of our work.

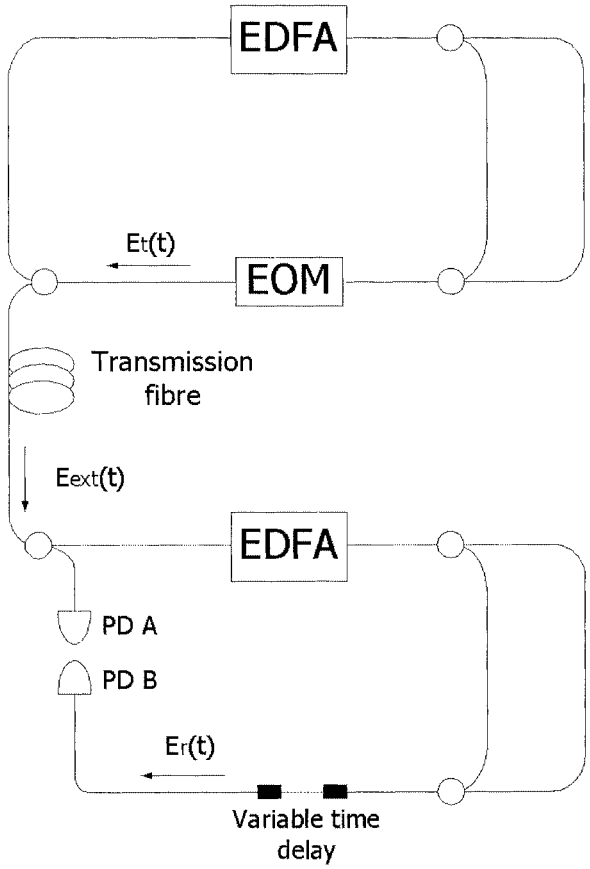

Fig. 1. Diagram of communication by synchronizing two chaotic EDFRLs. PD: photodiode; EOM: electrooptical modulator.

II. Theory Models

Fig. 1 shows the open-loop structure widely studied in the experiments [6], [7], [10], [12]. The transmitter consists of an EDFRL and an electrooptical modulator (EOM). The electric field circulating in the transmitter laser is $E_t(t)$, which is modulated by the message signal $m(t)$. An output coupler directs a part of $E_t(t)$ out of the ring and into the transmission fiber. The remaining light continues to circulate around the ring. At the end of the transmission fiber of L km, the chaotic output becomes $E_{\text{ext}}(t)$, which is injected into the receiver ring. In the receiver, the light is split again. One part of the signal is directly detected by photodiode A. The remaining part passes through the receiver with a variable time delay device and detected by photodiode B as $E_r(t)$. The variable time delay device can be adjusted so that the receiver path length is equal to the transmitter. In this way, the receiver chaos at photodiode B will be synchronized with the transmitter chaos $E_{\text{ext}}(t)$, which has been distorted by the transmission fiber. In the receiver, the chaos detected by photodiode B E_r is delayed relative to the chaos detected by photodiode A E_{ext} by one round-trip. Thus if we denote $E_r = E$, then $E_{\text{ext}} = m(t+\tau_R)E$. For simplicity, we just take the waveform shape and ignore the relative amplitude of E_{ext} and E_r.

The encoding of the message $m(t)$ is conducted by amplitude shift keying (ASK) technique. This is done by an electrooptical modulator in the transmitter loop such that the modulated signal can be represented by $|E_t'(t)| = m(t)|E_t(t)|$, where $m = \sqrt{1+K}$ for a "1" bit and $m = \sqrt{1-K}$ for a "0" bit. K is a modulation parameter and should be small enough to maintain laser stability. In this paper, we set $K = 0.1$. The message can be recovered by comparing $|E_{\text{ext}}|^2$ with $|E_r|^2$. The decoded message is $m'(t) = \sqrt{|E_{\text{ext}}|^2/|E_r|^2}$.

We follow the EDFRL model developed by Abarbanel *et al.* [8] and Lewis *et al.* [9]. The doped fiber ring laser contains an optical amplifier composed of erbium-doped single-mode fiber of length l_A and a piece of passive fiber of length l_F. The length of the optical cavity is then $l_A + l_F$. The propagation of the electrical field $E(z,t) = \varepsilon(z,t)\,e^{i(k_0 z - \omega_0 t)}$ in the active medium can be described by

$$\frac{\partial \varepsilon_{x,y}(z,\tau)}{\partial z} = gn(\tau)\,\varepsilon_{x,y} + L_{x,y}\varepsilon_{x,y} + N_{x,y}\varepsilon_{x,y}. \quad (1)$$

The retarded time is given by $\tau = t - z/v_g$, where v_g is the group velocity of the waves. g is the gain parameter and $n(\tau)$ population inversion.

The linear operator $L_{x,y}$ includes the linear birefringence, group-velocity dispersion (GVD), and gain dispersion

$$L_{x,y} = \pm\frac{ik_0(n_x - n_y)}{2n_0} \mp \frac{\Delta}{n_0 c}i\omega - \frac{i}{2}\beta_2\omega^2 - \frac{gn(\tau)\,\omega^2 T_2^2}{1+\omega^2 T_2^2}. \quad (2)$$

The nonlinear operators are

$$\begin{aligned} N_x\varepsilon_x = i\chi_3 \Bigg\{ &\left(|\varepsilon_x(z,\tau)|^2 + \frac{2}{3}|\varepsilon_y(z,\tau)|^2\right) \\ &\cdot \varepsilon_x(z,\tau) + \frac{1}{3}\varepsilon_x^*(z,\tau)\,\varepsilon_y(z,\tau)^2 \Bigg\} \\ N_y\varepsilon_y = i\chi_3 \Bigg\{ &\left(|\varepsilon_y(z,\tau)|^2 + \frac{2}{3}|\varepsilon_x(z,\tau)|^2\right) \\ &\cdot \varepsilon_y(z,\tau) + \frac{1}{3}\varepsilon_y^*(z,\tau)\,\varepsilon_x(z,\tau)^2 \Bigg\} \end{aligned} \quad (3)$$

where $\Delta = n_0(n_x - n_y)$ is the differential birefringence. T_2 is the decay time of the fast fluctuations of polarization. The third-order nonlinearity χ_3 can be related to the nondimensional nonlinear phase shift ψ_{nl} experienced by a field as it passes through the fiber, which can be given by $\psi_{nl} = \chi_3\pi(l_A + l_F)/\lambda(P_a + 2P_b)$, where P_a and P_b are the optical powers in the parallel and perpendicular directions.

In Fig. 1, a second loop of passive fiber is added to the ring. A fraction α of the light enters this fiber. As this light reenters the main ring, it will experience birefringence described by a Jones matrix J_{loop} and a second time delay τ_D. In this paper, we choose $\alpha = 0.1$ and $\tau_D = 0.208\tau_R$.

The overall propagation map M_ε including all the passive and active parts of the ring is

$$\begin{aligned} &\varepsilon(t+\tau_R) \\ &= M_\varepsilon\{\varepsilon(t)\} \\ &= RJ_{PC}\lfloor(1-\alpha)P\{\varepsilon(t)\} + \alpha J_{\text{loop}}P\{\varepsilon(t+\tau_D)\}\rfloor. \end{aligned} \quad (4)$$

From left to right, the terms are polarization-dependent attenuation, $R = \text{diag}(R_x, R_y)$, the unitary Jones matrix for the

TABLE I
TYPICAL PARAMETERS FOR EDFRL SIMULATIONS

Quantity	Symbol	Value
Linear birefringence	$n_x - n_y$	1.8×10^{-6}
Pump strength	Q	2.4×10^{-2}
Gain term	$2gl_A$	1.35×10^{-2}
Round trip time	τ_R	100 ns
Excited state lifetime	T_1	10 ms
Polarization dephasing time	T_2	1ps
GVD coefficient	β_2	-20ps^2/km
Polarization controller	$\theta_1, \theta_2, \theta_3$	0.5,1.2,1.5
Absorption coefficients	R_x, R_y	0.90,0.91
Active fibre length	l_A	10m
Passive fibre length	l_F	10m
Nonlinear phase shift	ψ_{nl}	1.6×10^{-2}

polarization controller J_{PC}, and the propagator through the active medium P. The overall phase factor and Jones matrix of the passive fiber have been absorbed into J_{PC}.

The dynamics of the ring laser can be described by the evolution equations of electrical field $\varepsilon(t)$ and integrated population inversion $w(\tau) = l_A^{-1}\int_0^{l_A} n(z,\tau)\,dz$.

In the receiver, the dynamical equations are

$$\varepsilon_r(\tau+\tau_R) = M_\varepsilon\left(w_r(\tau), \varepsilon_{\text{ext}}(\tau)\right) \tag{5}$$

$$\frac{dw_r(\tau)}{d\tau} = Q - \frac{\tau_R}{T_1}\left\{w_r(\tau) + 1 + |\varepsilon_{\text{ext}}(\tau)|^2\left(e^{2gl_A w_r(\tau)} - 1\right)\right\}. \tag{6}$$

The detailed numerical model can be found in [8]. We use similar parameters given in [8] and [9] for the EDFRL simulations, which are listed in Table I.

In the following calculations, we set 20 000 points around the ring to sample the electric field. This corresponds to a time resolution of 0.005 ns. We should be able to resolve fluctuations in electric field up to 200 GHz.

The propagation along the transmission fiber connecting the transmitter and the receiver is described by the nonlinear Schrödinger equation [14]

$$j\frac{\partial E}{\partial z} = -\frac{j}{2}\Gamma E + \frac{1}{2}\beta_2\frac{\partial^2 E}{\partial T^2} - \gamma|E|^2 E + \xi(z,T)\,\delta(z - nL_a). \tag{7}$$

Here $E(z,T)$ is the complex slowly varying amplitude field, z is the propagation distance, and T is the time measured in a reference frame moving at group velocity. γ is the nonlinear parameter that takes account of optical Kerr effect. Γ is the fiber loss. β_2 is the second-order dispersion parameter. $\xi(z,T)$ is amplifier noise introduced into the transmission fiber periodically at every lump amplifier. δ represents Dirac's delta function. $n = 1,2,3$ and L_a is amplifier spacing set as 60 km in this paper. In the simulation, we add to each spectral component of the transmitted field an independent noise term whose real and imaginary parts are independent Gaussian variables with variance [15]$\sigma^2 = n_{sp}h\nu(G-1)\Delta\nu/2$. G is the amplifier gain to compensate transmission loss. n_{sp} accounts for incomplete population inversion. h is Planck's constant, ν is the carrier frequency, and $\Delta\nu$ is the bandwidth occupied by each discrete Fourier spectrum component. The amplifier noise figure (NF) is considered to be 5 dB by setting $n_{sp} = 1.6$, since $NF = 10\log_{10} 2n_{sp}$.

III. SIMULATION RESULTS AND DISCUSSIONS

The decoding scheme is illustrated in Fig. 2. E_{ext} and E_r are first converted into two electrical signals by means of the photodiodes. These photodiodes must have a sampling bandwidth at least equal to the message bit rate. Electrical filters can also be added after the photodiodes, in the form of a second-order low-pass Butterworth filter (called filter 1) with a bandwidth of 1.3 BR [13] (here BR is the bit rate of the message). We choose this value since it can preserve the modulation information as well as remove the fast fluctuations caused by the detrimental effects in the transmission fiber. After the division of the two signals for extracting the message, another Butterworth filter (filter 2, with a bandwidth of 0.8 BR) is used to refine the recovered message. The system performance can be quantitatively evaluated by means of the EOP, which is defined as $10\log(a/b)$, where a and b are the maximum eye openings measured for the decoded message without and with transmission.

We consider a transmission fiber consisting of a combination of a conventional single-mode fiber (SMF, $\Gamma_1 = 0.2$ dB/km, $\beta_{21} = -20$ ps^2/km, and $\gamma_1 = 1.3$/W/km) and a dispersion-compensating fiber (DCF, $\Gamma_2 = 0.5$ dB/km,

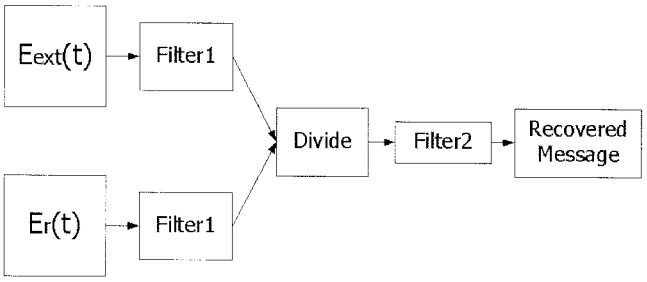

Fig. 2. The scheme of decoding message.

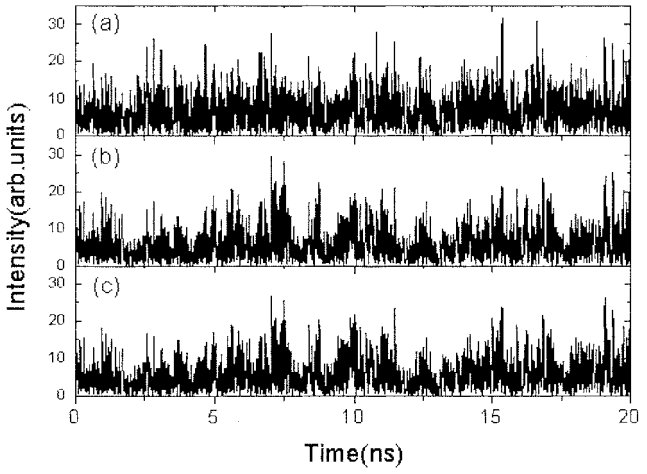

Fig. 3. Chaotic evolution of the transmitter and the receiver sampled at 200 GHz. The two EDFRLs are linked by a dispersion-compensated fiber of 120 km. The transmission power is set as $P_{\rm av} = 0$ dBm. (a) Typical output from the transmitter without encoding message; (b) typical output of the transmitter (E_t) after encoding digital message at a bit rate of 3.12 Gb/s; (c) output of the receiver (E_r).

$\beta_{22} = 100\ \text{ps}^2/\text{km}$, and $\gamma_2 = 3.5/\text{W/km}$). At first, we ignore the amplifier noise and consider only the effect due to the transmission fiber. Since the dispersion effect of the fiber is removed by compensation, the only detrimental effect left to be considered is its nonlinearity. If the transmission fiber is periodically amplified, the average transmission power at the output of the amplifier can be characterized by $P_{\rm av}$. Fig. 3(a) shows the temporal behavior of the transmitter chaos without modulation and Fig. 3(b) is for the case when the chaos is modulated with a digital message at 3.12 Gb/s. The modulation will throw the laser field into a totally different chaos trajectory, so Fig. 3(b) is quite different compared with Fig. 3(a). The receiver chaos is shown in Fig. 3(c), which, as can be seen, is synchronized to the modulated transmitter chaos given in Fig. 3(b), enabling the encoded message to be recovered by comparing them. It should be noted that in the receiver, the chaos is not modulated by any digital message, although it looks to be similar to the chaos shown in Fig. 3(b). The reason for the superficial resemblance is due to the small amplitude of the digital message encoded in the transmitter chaos.

The decoded message from the receiver is showed in Fig. 4(b). It is similar to the original message given in Fig. 4(a) except for the sharp fast oscillations. These oscillations come from the small differences in the time traces of the transmitter output before and after 120-km propagation. The quality of the

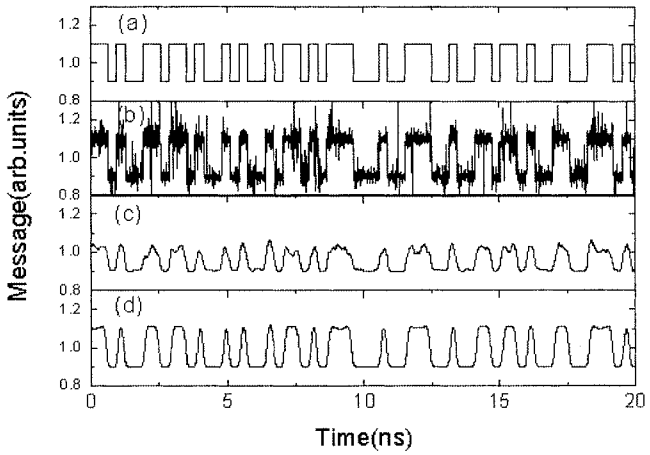

Fig. 4. Message encoding and decoding; the parameters are the same as in Fig. 3. (a) Encoded digital message of 3.12 Gb/s; (b) decoded message without filter 1 and filter 2; (c) recovered message with only filter 2 used; and (d) recovered message with both filter 1 and filter 2 used.

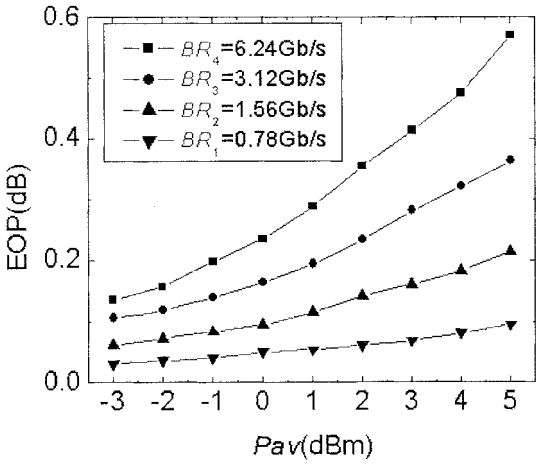

Fig. 5. EOP versus average transmission power after 120-km transmission for several bit rates (only considering fiber nonlinearity effect).

decoded message can be improved by using the appropriate bandpass filter to eliminate the fast oscillations. Filter 1 can remove these oscillations before the division process. In Fig. 4(d), we can see the filtered message is quite good compared with the input message [Fig. 4(a)].

The system performances influenced by the fiber nonlinearity for several bit rates are displayed in Figs. 5 and 6. It is clear that the EOP increases with both the average transmission power and transmission distance. For example, less than 0.8-dB penalty is observed for 6.24-Gb/s message propagating over 300 km at $P_{\rm av} = 0$ dBm.

Filter 1 is also useful when eliminating the influence of amplifier noise. Fig. 7 shows the decoded message before filter 2. Fig. 8 gives the corresponding eye diagrams. Obviously, the fast oscillations are reduced when filter 1 is used. The smallest EOP is obtained from Fig. 8(c) when filter 1 is sampled at 1.3 BR_2.

Fig. 9 displays the EOP degradation at different average transmission power under the influence of amplifier noise. The transmission distance is 60 km, which means the amplifier noise with $\text{NF} = 5$ dB is introduced. Considerable increase of EOP is found when the message bit rate is $\text{BR}_3 = 3.12$ Gb/s. We believe the

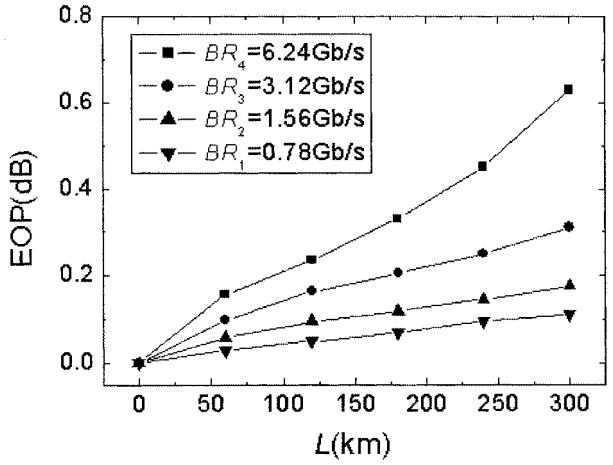

Fig. 6. Deterioration of EOP with transmission distance increasing due to fiber nonlinearity. $p_{\rm av} = 0$ dBm.

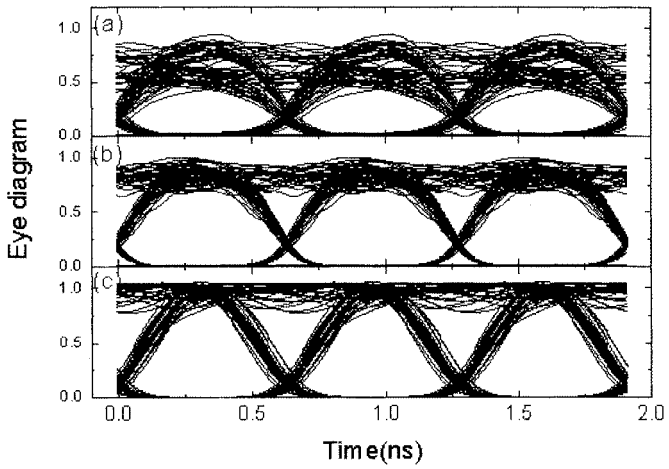

Fig. 8. Eye diagram at three different cases. The parameters in each case are the same as in Fig. 7. EOP values are (a) 1.88, (b) 0.72, and (c) 0.37, respectively.

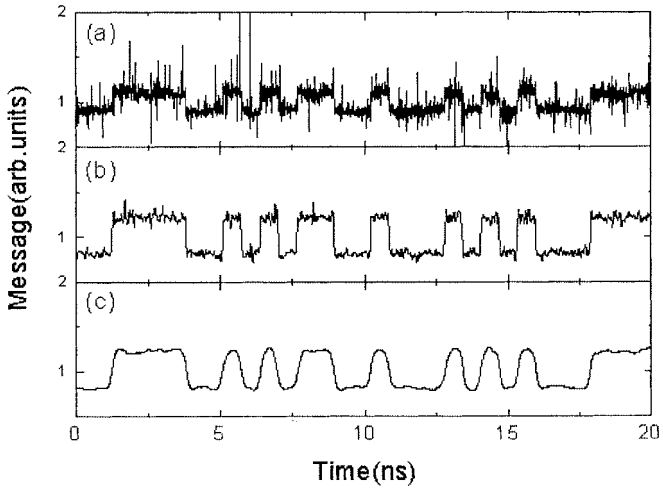

Fig. 7. Decoded message before filter 2. The bit rate is $\mathrm{BR}_2 = 1.28$ Gb/s with $P_{\rm av} = 0$ dBm. The fiber length is 60 km and only the effect of amplifier noise is taken into account. (a) Without filter 1; (b) with filter 1 sampled at 5.0 BR_2; and (c) with filter 1 sampled at 1.3 BR_2.

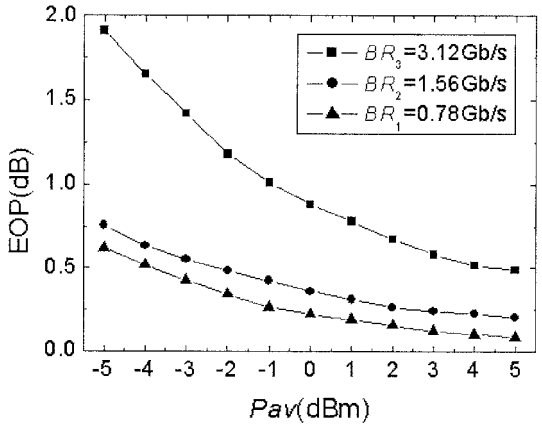

Fig. 9. EOP versus average transmission power after 60-km transmission for several bit rates (only considering amplifier noise).

optimum transmission power may be chosen to balance the influence of both amplifier noise and fiber nonlinearity.

IV. Comparison Between Different Transmission Fibers

In Section III, we used EOP as a figure of merit. However, the system performance can also be described by the more important parameter BER, which is given by [16]: BER $\approx \exp\left(-Q^2/2\right)/\sqrt{2\pi}Q$, where Q is given by $Q = \left(\langle 1\rangle - \langle 0\rangle\right)/\left(\sigma_1 + \sigma_0\right)$. Here $\langle 1\rangle$ and $\langle 0\rangle$ are the mean intensity for binary 1 and 0 states, while σ_1 and σ_0 are the corresponding standard deviations.

In the above section, we assumed a transmission fiber completely dispersion-compensated. However, one would like to know the system performance when the fiber dispersion is not completely compensated. So we examine the BER degradation with the residual fiber dispersion in Fig. 10. Both fiber nonlinearity and amplifier noise are excluded. It is clear that one must make the residual dispersion as small as possible in order to realize high-speed message transmission. Fig. 10 can be a criterion used to evaluate the influence of fiber dispersion on chaotic encoded communication.

Now we consider three different transmission fibers: a) single-mode fiber; b) dispersion-compensated fiber consisting of a single-mode fiber and a dispersion-compensating fiber; and c) dispersion-shifted fiber (DSF, $\Gamma = 0.2$ dB/km, $\beta_2 = -0.1$ ps^2/km, and $\gamma = 1.5$/W/km).

When dispersion is not compensated, i.e., for the case of typical single-mode fiber communication, Fig. 11 illustrates BER versus average transmission power at different transmission distances. The amplifier noise, fiber dispersion, and nonlinearity are all taken into account. The residual dispersion $\beta_2 L$ is 1200 ps^2 for 60 km and 2400 ps^2 for 120 km. So the errors are mainly induced by fiber dispersion. From Fig. 10, faithful communication at bit rate BR_3 and BR_2 is impossible. So only the case of BR_1 is shown. Even in this case, acceptable BER is obtained for length less than 60 km.

For the case of b) and c), Fig. 12 shows that there exists the optimum transmission power that can balance the effect of amplifier noise and fiber nonlinearity. For example, the smallest BER can be achieved at $P_{\rm av} = 3$ dBm for a dispersion-compensated

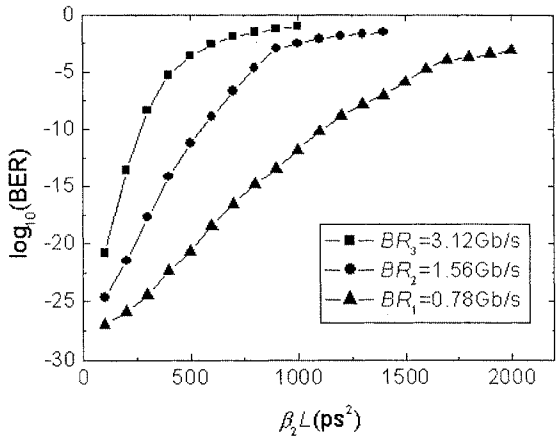

Fig. 10. BER versus residual dispersion $\beta_2 L$ in the transmission fiber for different bit rates. L is the transmission distance.

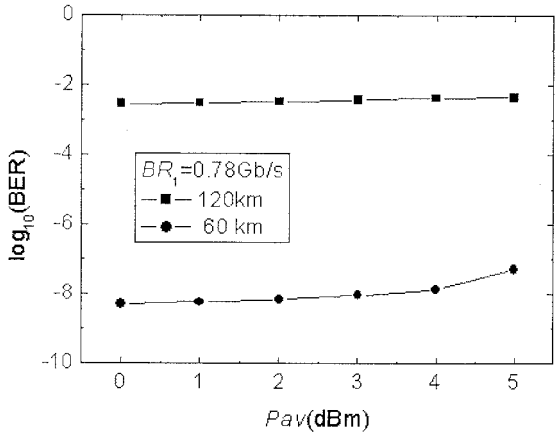

Fig. 11. BER versus average transmission power $P_{\rm av}$ in single-mode fiber transmission.

fiber and at $P_{\rm av} = 2$ dBm for a dispersion-shifted fiber. Since amplifier gains at spacing length 60 km are 15 and 12 dB for b) and c), respectively, the dispersion-compensated fiber suffers more noise effect. Moreover, from the criterion in Fig. 10, the residual dispersion in a dispersion-shifted fiber is not a problem for hundreds of kilometers transmission. So in general, the dispersion-shifted fiber shows better performance than for case b). However, with the transmission power increasing, system performance degrades more rapidly for the DSF case, especially when the encoded communication has higher bit rate $\rm BR_3$. This is not surprising since in case b) the transmitted field is broadened by SMF and then compressed by DCF, while in case c), it only slightly broadened due to the small dispersion of DSF. Thus fiber nonlinearity effect is more serious in the DSF.

Figs. 13 and 14 display the deterioration of the BER as a function of transmission distance at different bit rates for cases b) and c), respectively. In each case $P_{\rm av}$ is set at its optimum value. In these figures, amplifier noise, fiber nonlinearity, and dispersion have been taken into account. It can be seen that gigabit/second chaos communication can be realized up to several hundred kilometers.

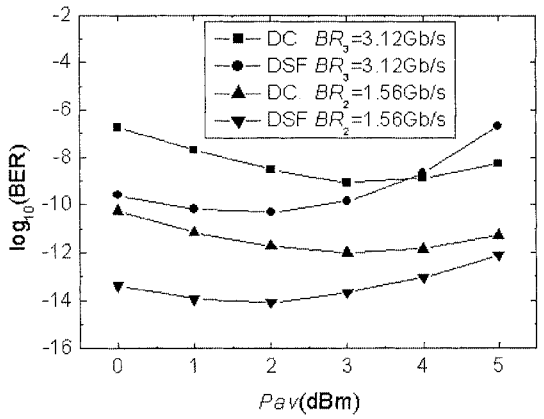

Fig. 12. BER versus the average transmission power $P_{\rm av}$ in dispersion-compensated (DC) fiber and DSF transmission. The transmission distance is 240 km.

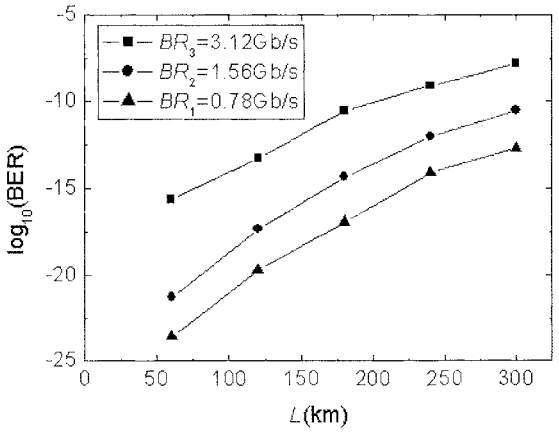

Fig. 13. BER deterioration with transmission distance increasing at different message bit rates in a dispersion-compensated fiber. $P_{\rm av} = 3$ dBm.

V. Transmission Performance When Using Closed-Loop Structure

The above discussions are based on the open-loop structure, which is often employed in the previous experiments [6], [7], [10], [12]. However a closed-loop scheme is also of interest and deserves further study. In [9], the closed-loop structure with partially modulated branch is suggested. The setup is shown schematically in Fig. 15. In the transmitter, before the laser chaos is modulated, the optical field is split in a proportion $c : 1 - c$. The c branch in the transmitter is electrooptically modulated, while the unmodulated $1 - c$ branch is included to achieve synchronization for coupling in the range of $0 < c < 1$. For $c = 1$, the unmodulated branch is not needed; it becomes the open-loop scheme (a single-loop ring). After L km propagation, the transmitted field $cm\varepsilon_t$ becomes $cm'\varepsilon_t'$ and injects into the receiver. The equations for the two coupled lasers are

For the transmitter laser

$$\varepsilon_t(\tau + \tau_R) = M_\varepsilon\left(w_t(\tau), (cm + 1 - c)\,\varepsilon_t(\tau)\right) \tag{8}$$

$$\frac{dw_t(\tau)}{d\tau} = Q - \frac{\tau_R}{T_1}\left\{w_t(\tau) + 1 + \left|(cm + 1 - c)\,\varepsilon_t(\tau)\right|^2 \cdot \left(e^{2gl_A w_t(\tau)} - 1\right)\right\}. \tag{9}$$

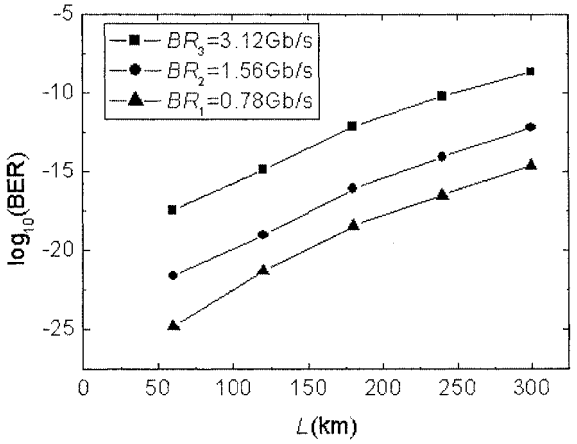

Fig. 14. BER deterioration with transmission distance increasing at different message bit rates in a DSF. The average transmission power is $P_{\rm av} = 2$ dBm.

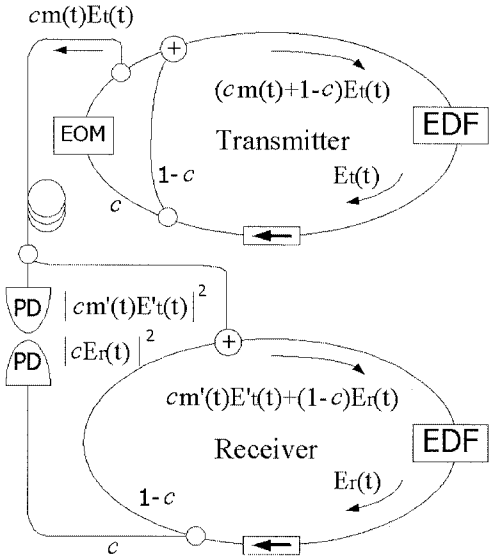

Fig. 15. Encoded communication employing closed-loop scheme with partial modulation.

For the receiver laser

$$\varepsilon_r(\tau+\tau_R) = M_\varepsilon\left(w_r(\tau), cm'\varepsilon_t' + (1-c)\,\varepsilon_r(\tau)\right) \tag{10}$$

$$\frac{dw_r(\tau)}{d\tau} = Q - \frac{\tau_R}{T_1}\left\{w_r(\tau) + 1 + \left|cm'\varepsilon_t' + (1-c)\,\varepsilon_r(\tau)\right|^2 \cdot \left(e^{2gl_A w_r(\tau)} - 1\right)\right\}. \tag{11}$$

The message can be recovered by comparing the injected field and the receiver output

$$m'(t) = \sqrt{\frac{\left|cm'(t)\,E_t'\right|^2}{\left|cE_r\right|^2}} = \sqrt{\frac{\left|cm(t)\,E_t + \Delta E_t\right|^2}{\left|cE_r\right|^2}}.$$

ΔE_t takes into account the total distortion of the injected field. Although the coupling strength c can be different, cmE_t experiences the same detrimental effects such as amplifier noise, fiber nonlinearity, and dispersion. In other words, the channel introduces the same level of distortion ΔE_t regardless of coupling c, once the transmission power is set. We choose DSF as a transmission fiber and set $P_{\rm av} = 2$ dBm. The performance of chaotic EDFRL system with closed-loop structure is demonstrated for various c values in Fig. 16. Obviously the BER is smaller for larger coupling and the best performance is achieved by the open-loop structure ($c = 1$). For the case of $c < 1$, a receiver with an open loop cannot realize faithful communication since a time-delay version of injected field is not enough to recover the message and the synchronized chaos in the receiver is needed. So it seems that a closed-loop structure has enhanced security compared with an open-loop one. However, we believe that the security is actually improved by the complex structure of the transmitter. For example, in Fig. 1, although the open-loop scheme is used to recover the message, the second passive loop in the transmitter provides more physical parameters that the receiver must match. Thus a dual-ring transmitter has better security than a single-ring transmitter, since the receiver must employ a similar structure as its corresponding transmitter.

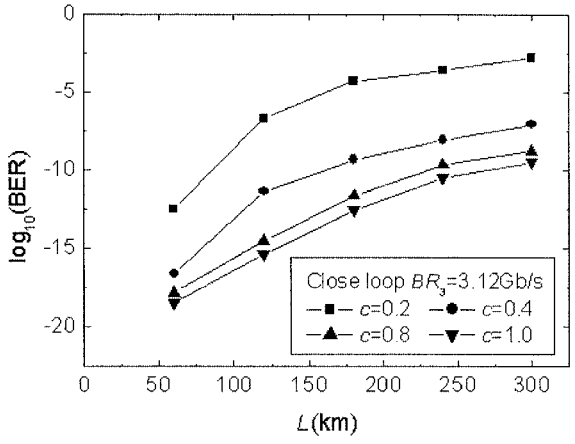

Fig. 16. BER deterioration with transmission distance increasing when using a closed-loop scheme illustrated in Fig. 15. $c = 1.0$ corresponds to the open-loop structure.

VI. Maximum Message Bit Rate in a Chaos Communication System

Now we address the question: what is the maximum bit rate that EDFRL chaos system can support? To answer this question, we plot the power spectrum of a typical output of EDFRL with parameters given in Table I. Fig. 17 shows the broad spectrum of the chaos generated, which has been estimated to have a bandwidth of about 50 GHz. This would appear to be the maximum message bit rate allowed.

However, an acceptable message bit rate should not be too close to the bandwidth of the EDFRL chaos. Fig. 18 displays the decoded message at three high bit rates, and Fig. 19 shows the time series of the chaos output at the corresponding sampling bandwidths. Fig. 18(a) shows that filter 1 is efficient for the case of $\rm BR_3$. However, even without detrimental effect, some distortions are still seen in Fig. 18(b) at $\rm BR_4 = 6.24$ Gb/s and more serious in Fig. 18(c) at $\rm BR_5 = 12.48$ Gb/s. The reason is

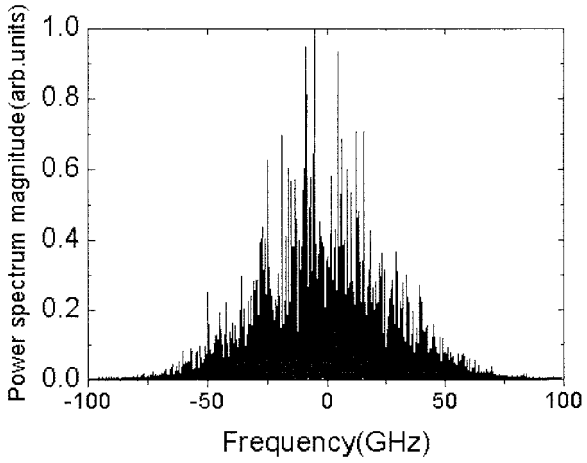

Fig. 17. Typical power spectrum of the transmitter without modulation at $\psi_{nl} = 1.6 \times 10^{-2}$.

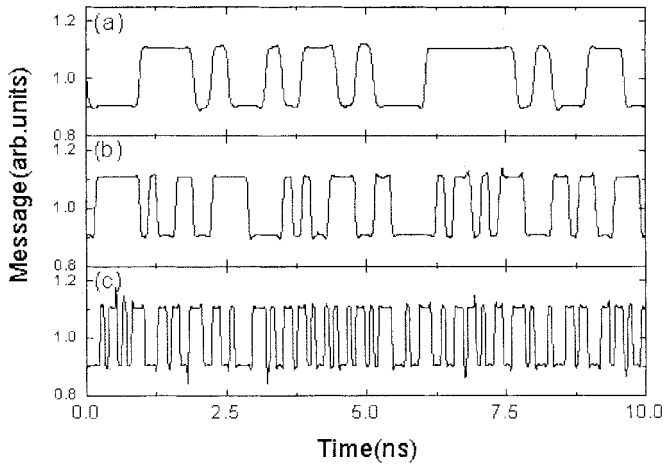

Fig. 18. Decoded message before filter 2. No detrimental effect is considered. (a) $BR_3 = 3.12$ Gb/s, sampled by filter 1 at 1.3 BR_3, (b) $BR_4 = 6.24$ Gb/s, sampled by filter 1 at 1.3 BR_4, and (c) $BR_5 = 12.48$ Gb/s, sampled by filter 1 at 1.3 BR_5.

that the sampling bandwidth (or the bit rate) is on the same scale with the chaos carrier intensity fluctuation. This can be seen from Fig. 19(a)–(c), which shows the sampled chaos intensity at three bandwidths. The filter itself will give some distortion. In other words, the filter is no longer efficient to remove noise-induced errors. The eye diagram is plotted in Fig. 20 for the case of $BR_5 = 12.48$ Gb/s with only amplifier noise considered. P_{av} is set to 0 dBm in a dispersion–compensated fiber and the transmission distance is 60 km. The EOP value is as large as 4.73 and the BER is as low as 10^{-5}.

We can therefore expect that higher message bit rate can be transmitted in a chaotic carrier with larger bandwidth. Abarbanel [8] showed that the chaos in EDFRL originates from Kerr effect in the fiber. The Lyapunov exponent increases with ψ_{nl}, which is proportional to χ_3 that in turn is related to the Kerr coefficient. So if we set a smaller value of ψ_{nl}, we should obtain a slower chaotic oscillation and less bandwidth. Fig. 21 displays the power spectrum at $\psi_{nl} = 0.4 \times 10^{-2}$. The bandwidth is estimated to be 25 GHz. Thus the maximum bit rate it can convey should be lower than that in the case of $\psi_{nl} = 1.6 \times 10^{-2}$. Fig. 22 shows such a bit rate limitation when the message is encoded at $BR_5 = 12.48$ Gb/s. In Fig. 22(a), we can see that the intensity drops close to zero at many points. Large errors will be produced due to noise fluctuation at these points. Filter 1 is not useful since it will cause large distortion as shown in Fig. 22(c). This is because the message bit rate BR_5 is too close to the chaos bandwidth. In this case, even a filter cannot be useful. Although only amplifier noise is considered, the corresponding eye diagram is nearly closed, as seen in Fig. 23.

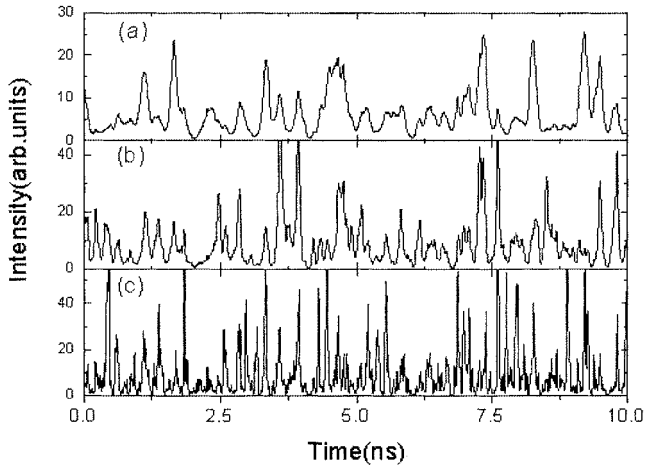

Fig. 19. Time series of the transmitter output sampled at (a) 1.3 BR_3, (b) 1.3 BR_4, and (c) 1.3 BR_5.

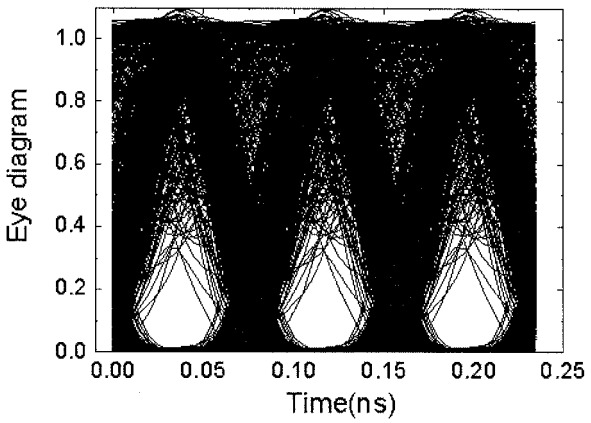

Fig. 20. Eye diagram when encoding message at bit rate BR_5. The transmission distance is 60 km. $P_{\text{av}} = 0$ dBm and $\psi_{nl} = 1.6 \times 10^{-2}$.

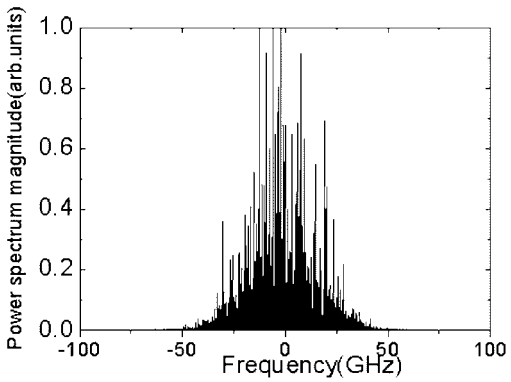

Fig. 21. Typical power spectrum of the transmitter without modulation at $\psi_{nl} = 0.4 \times 10^{-2}$.

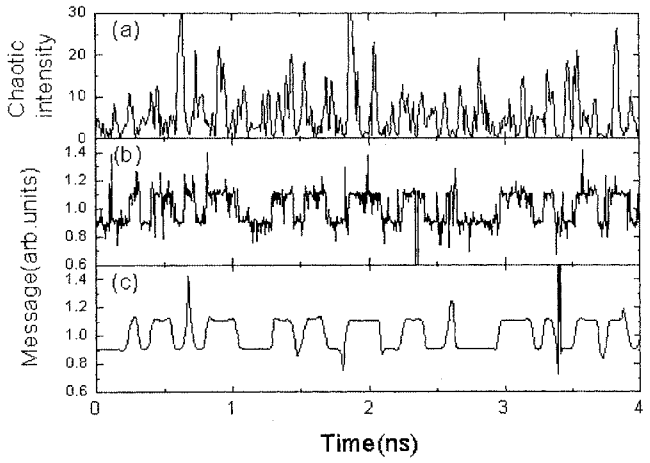

Fig. 22. Bit rate limitation when encoding message $BR_5 = 12.48$ Gb/s. The transmission distance is 60 km. $P_{av} = 0$ dBm and $\psi_{nl} = 0.4 \times 10^{-2}$. (a) Chaotic intensity of the receiver input sampled at 1.3 BR_5, (b) decoded message before filter 2 (without filter 1, amplifier noise figure NF $= 5$ dB), and (c) decoded message before filter 2 (with filter 1 sampled at 1.3 BR_5, no detrimental effect).

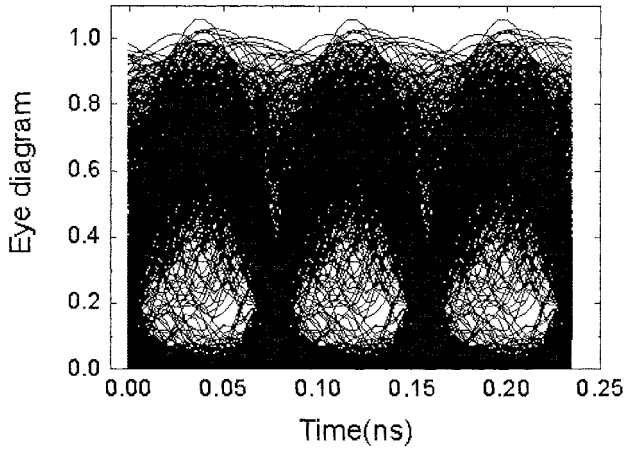

Fig. 23. Closed eye diagram when encoding message BR_5 with $NF = 5$ dB and $\psi_{nl} = 0.4 \times 10^{-2}$.

Therefore, to increase the maximum message bit rate, we need to increase the chaos bandwidth. This in turn depends on the parameters of the EDFRL. Since it has been determined that chaos arises from the fiber nonlinearity, we can increase the pump power, which has an effect of increasing the nonlinearity, and hence the chaos bandwidth. Furthermore, we also note that the chaos bandwidth increases with the Lyapunov exponent value, which in turn depends on various laser parameters. For example, the polarization-dependent attenuation difference ΔR and linear birefringence Δn will break transmission symmetry and increase Lyapunov exponent value. The introduction of the second loop length τ_D in the EDFRL and the corresponding portion α of light entering this loop also profoundly influence the Lyapunov exponent value. Thus one can choose these parameters of the EDFRL appropriately to yield the largest Lyapunov exponent that in turn produces the maximum chaos bandwidth.

VII. Conclusion

In this paper, we have numerically studied the system performance degradation of gigabit/second digital secure communication due to the detrimental effects in the transmission fiber. The residual fiber dispersion must remain as small as possible to realize high-bit-rate chaos communication. The optimum transmission power exists that can balance the effect of fiber nonlinearity and amplifier noise. The system performances employing different transmission fibers such as single-mode fiber, dispersion-compensated fiber, and dispersion-shifted fiber are thoroughly discussed. When embedded in the chaotic EDFRL laser, the gigabit/second message can be transmitted over several hundred kilometers without excessive deterioration of BER. The maximum message bandwidth is determined by the bandwidth of the chaos that is in turn determined by the physical parameters in the EDFRL.

Acknowledgment

The authors would like to thank M. Kennel, G. VanWiggeren, and M. Buhl for their valuable discussions.

References

[1] L. M. Pecora and T. L. Carroll, "Synchronization in chaotic systems," *Phys. Rev. Lett.*, vol. 64, no. 8, pp. 821–824, Feb. 1990.
[2] P. Colet and R. Roy, "Digital communication with synchronized chaotic lasers," *Opt. Lett.*, vol. 19, no. 24, pp. 2056–2058, Dec. 1994.
[3] T. Sugawara, M. Tachikawa, T. Tsukamoto, and T. Shimizu, "Observation of synchronization in laser chaos," *Phys. Rev. Lett.*, vol. 72, no. 22, pp. 3502–3505, May 1994.
[4] C. R. Mirasso, P. Colet, and P. Garcia-Fernandez, "Synchronization of chaotic semiconductor lasers: Application to encoded communication," *IEEE Photon. Technol. Lett.*, vol. 8, pp. 299–301, Feb. 1996.
[5] L. G. Luo and P. L. Chu, "Optical secure communication with chaotic erbium doped fiber lasers," *J. Opt. Soc. Amer. B*, vol. 15, no. 10, pp. 2524–2530, Oct. 1998.
[6] G. D. VanWiggeren and R. Roy, "Communication with chaotic lasers," *Science*, vol. 279, pp. 1198–1200, Feb. 1998.
[7] ——, "Optical communication with chaotic waveform," *Phys. Rev. Lett.*, vol. 81, no. 16, pp. 3547–3549, Oct. 1998.
[8] H. D. I. Abarbanel, M. B. Kennel, M. Bhul, and C. T. Lewis, "Chaotic dynamics in erbium doped fiber ring laser," *Phys. Rev. A*, vol. 60, no. 3, pp. 2360–2374, Sep. 1999.
[9] C. T. Lewis, H. D. I. Abarbanel, M. B. Kennel, M. Bhul, and L. Illing, "Synchronization of chaotic oscillations in doped fiber ring lasers," *Phys. Rev. E*, vol. 63 016 215, 2000.
[10] L. G. Luo, P. L. Chu, and H. F. Liu, "1 GHz optical communication system using chaos in erbium-doped fiber lasers," *IEEE Photon. Technol. Lett.*, vol. 12, pp. 269–271, Mar. 2000.
[11] S. Kim, B. Lee, and D. H. Kim, "Experiments on chaos synchronization in two separate erbium-doped fiber lasers," *IEEE Photon. Technol. Lett.*, vol. 13, pp. 290–292, Apr. 2001.
[12] G. D. VanWiggeren and R. Roy, "Chaotic communication using time-delayed optical systems," *Int. J Bifurcation Chaos*, vol. 9, no. 11, pp. 2129–2156, Nov. 1999.
[13] A. Sanchez-Diaz, C. R. Mirasso, P. Colet, and P. Garcia-Fernandez, "Encoded Gbit/s digital communications with synchronized chaotic semiconductor lasers," *IEEE J. Quantum Electron.*, vol. 35, pp. 292–297, Mar. 1999.
[14] G. P. Agrawal, *Nonlinear Fiber Optics*. San Diego, CA: Acadamic, 1989.
[15] F. Matera and M. Settembre, "Comparison of the performance of optically amplified transmission systems," *J. Lightwave Technol.*, vol. 14, no. 1, pp. 1–12, 1996.
[16] N. A. Olsson, "Lightwave systems with optical amplifiers," *J. Lightwave Technol.*, vol. 7, no. 7, pp. 1071–1082, 1989.

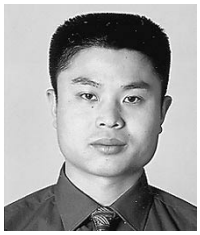

Fan Zhang was born in Kaifeng, Henan Province, China, in 1975. He received the M.Sc. degree from Xi'an Institute of Optics and Precision Mechanics, Chinese Academy of Science, China, in 1999 and the Ph.D. degree from Beijing University of Posts and Telecommunications, Beijing, China, in 2002.

Since 2002, he has been a Senior Research Associate with Optoelectronics Research Centre, City University of Hong Kong, working on chaos communication based on fiber ring lasers. His research interests are in the areas of high-speed optical communication systems and networks, optical packet switching, and optical secure communication systems.

Pak L. Chu (M'78) was born in China. He received the B.E. (Hons.), M.E., and Ph.D. degrees from the University of New South Wales, Sydney, Australia.

After graduation, he spent a year with AWA Pty. Ltd., Sydney, working on microwave antenna research and development. A year later, he returned to the School of Electrical Engineering, University of New South Wales, as a Tutor and then Lecturer, Senior Lecturer, Associate Professor, and finally Professor and Head of the Optical Communications Group. In July 2001, he returned to Hong Kong as the Director of the Optoelectronics Research Centre and Chair Professor of the Department of Electronic Engineering, City University of Hong Kong. His research interests are in optical communication, optical fiber technology, optical waveguide technology, electromagnetic theory, plasma oscillations, and wave propagation in nonlinear media. He has published more than 400 papers in international journals and conferences in these areas.

Dr. Chu is a Fellow of the Australian Academy of Technological Sciences and Engineering, a Fellow of the Optical Society of America (OSA), and a Fellow of the Institution of Engineers Australia. He received the Centenary Medal from the Prime Minister's Department of Australia in 2003 for his contributions in optical communications.